EARTHQUAKE ENGINEERING AND STRUCTURAL DYNAMICS
Earthquake Engng. Struct. Dyn. **28**, 857–878 (1999)

DYNAMIC TESTING AND SYSTEM IDENTIFICATION OF A MULTI-SPAN HIGHWAY BRIDGE

C. S. HUANG[1,*,†], Y. B. YANG[2,‡], L. Y. LU[1,§] AND C. H. CHEN[3,‖]

[1] *National Center for Research on Earthquake Engineering, 200, Sec. 3, Hsinhai Rd., Taipei, Taiwan, R.O.C.*
[2] *Department of Civil Engineering, National Taiwan University, Taipei, Taiwan, R.O.C.*
[3] *Department of Civil Engineering, Kao Yoan College, Kaohsiung, Taiwan, R.O.C.*

SUMMARY

A simple and effective procedure for conducting the free vibration test on highway bridges is presented. The impulsive force in each direction is generated by a loaded truck that either stops suddenly or falls down from a rigid block. The feasibility of the procedure is demonstrated in identification of the dynamic properties, i.e. the vibration frequencies, mode shapes, and damping ratios, of a three-span box-girder concrete bridge using the Ibrahim Time-Domain (ITD) technique. Up to 14 modes have been identified for the present case. For the purpose of verification, ambient vibration tests were also carried out, with the data processed by the random decrement (Randomdec) technique to yield the free vibration response, followed by the ITD technique. The dynamic properties identified from the two types of test correlate very well with each other, indicating the validity of each procedure described herein. Although many more modes can be identified from the free vibration test because of the higher quality of data produced, the easiness and general applicability of the ambient vibration test can still be appreciated. A comparison of the experimental results with those by the finite element method indicated a lesser degree of correlation, implying that the finite element model adopted in design requires further refinement, say, through a more realistic evaluation of the boundary conditions, geometric and material properties of the bridge. Copyright © 1999 John Wiley & Sons Ltd.

KEY WORDS: multi-span bridge; free vibration test; ambient vibration test; system identification

1. INTRODUCTION

Performing field experiments is the most reliable means of determining the dynamic characteristics of a structural system including the natural frequencies, mode shapes, and damping ratios. These structural parameters are very useful for reevaluating the original design, for active control, for calibrating the analytical model and even for damage assessment. There are several typical

* Correspondence to: C. S. Huang, National Center for Research on Earthquake Engineering, 200, Sec. 3, Hsinhai Road, Taipei, Taiwan, R.O.C. E-mail: cshuang@email.ncree.gov.tw
† Research Fellow
‡ Professor
§ Associate Research Fellow
‖ Assistant Professor

Contract/grant sponsor: Taiwan-Area National Freeway Bureau, Ministry of Transportation and Communications

CCC 0098–8847/99/080857–22$17·50

Received 7 July 1998
Revised 21 December 1998

ways for conducting field experiments, ranging from the forced vibration test through use of the eccentric mass exciter[1] or the electrohydraulic shaker,[2] free vibration test using the pendulum device,[3] test vehicle,[4] or by imposing the initial displacements,[5,6] to the ambient vibration test[7,8] considering the disturbance of normal traffic or natural forces such as wind or earth tremble. Each test procedure has its own advantages. Generally speaking, ambient vibration test provides an easily applicable method in the field, while forced and free vibration tests provide better results because of the use of well-defined input. LaShomb *et al.*[9] performed a detailed review of the field dynamic tests for bridges. Mazurek[10] and Yang *et al.*[11] gave a comprehensive review on the application of ambient vibration tests to bridges. Paultre *et al.*[12] summarized some of the field studies on bridge–vehicle interaction.

In the present work, to identify the dynamic characteristics of a multi-span freeway bridge, we used both the ambient vibration test and free vibration test along with a truck to generate the impulsive forces. The latter test was briefly noted by Paultre *et al.*[12] The purpose of the paper is twofold: (1) to present the procedure of free vibration test in detail; (2) to demonstrate its applicability to such a multi-span freeway bridge. The present testing procedure is characterized by the fact that it is easy to set up, while producing data of good quality.

Regarding analysing measured data, the techniques in frequency domain appear to be most frequently used. Although spectral analysis may provide an easy method for identifying the natural frequencies of a system, identification of the damping ratios and mode shapes are not as straightforward, especially for highly damped systems and systems with severe modal interference. These drawbacks can be somewhat overcome by using wavelet transform instead of conventional FFT-based approach.[13–15]

In the present study, a technique in time domain that combines the random decrement (Randomdec) technique[16] and the Ibrahim time-domain identification (ITD) technique[17] will be used to analyse the data collected from ambient vibration test. This procedure is quite straightforward and simple because the measured responses in time domain are directly used without doing any transformation. Besides, the procedure is well established and has been successfully applied to identifying the dynamic characteristics of real structural systems.[18,19] The random decrement technique is applied to extracting the free vibration signals from the ambient vibration measurement. Then, the ITD technique is applied to extracting from the free vibration signals the natural frequencies, modal damping ratios, and mode shapes of the system. Huang *et al.*[19] proved that under certain circumstances, the Randomdec velocity or displacement signature of a linear time-unvaried system is equivalent to the free-decay behaviour of the system. However, in the field test for a multi-span highway bridge, the input conditions may not exactly satisfy the requirement for the equivalence between the Randomdec signature and free-decay response. With this in mind, the applicability of the present analysis procedure will be demonstrated by comparing the obtained results with those from independent free vibration tests. Finally, the natural frequencies and mode shapes identified from these two tests will be compared with those from the finite element analysis with discussion given concerning the accuracy of the results from the latter.

2. DESCRIPTION OF THE TESTED BRIDGE

The tested bridge is a unit of the northbound line of the newly constructed elevated freeway bridge system with a total length of about 21 km in the Taipei metropolitan area of Taiwan,

which is referred to as the Yuan-Shan bridge in this paper. This tested bridge consists of three-span continuous pre-stressed concrete box-girders with varying cross-sectional areas and is 360 m long in total. The bridge is about 27 m high above the ground level and the lengths of the three spans are 95, 155 and 110 m (see Figure 1). A typical cross-section of the bridge is also shown in Figure 1. The width of the deck is about 12·6 m, and the height of the box-girder is generally larger than 3·5 m. The tested bridge unit is supported by rollers in the longitudinal direction (identified as 'M' for 'movable' in the figure) but are constrained in the transverse and vertical directions at the two far ends. Meanwhile, it is rigidly supported by the two central columns (identified as 'R' for 'rigid' in the figure). Both of the two end spans of the tested unit are separated from the adjacent spans by expansion joints. It should be mentioned that the field tests for the bridge were performed right before the bridge was opened to the public.

3. FREE VIBRATION TEST

3.1. Generation of an impulsive force

In order to obtain the free-decay vibration response of the bridge, an impulsive force, which was generated by a loaded truck weighing about 14 tons, was imposed on the bridge. The force was repeatedly applied at the center point of the bridge deck of the middle span, i.e. the 155 m span (see Figure 1), in three orthogonal directions, namely, the longitudinal, transverse and vertical directions. The longitudinal force was applied by suddenly braking the truck at the desired location when the truck travelled along the centreline of the bridge deck at a specific speed. The transverse force was generated in the same way as that for the longitudinal force, except that the truck travelled in a direction with an inclined angle of 30° from the centerline of the deck (see Figure 2). The vertical force was generated by simply letting the rear wheels of the truck fall down from the top of a concrete block of 20 cm height at the desired location.

3.2. Instrumentation for measurement

When an impulsive force was applied for a specific direction, several highly sensitive sensors of the servo velocity type were used to measure the free vibration response of the bridge in that direction. The analogue sensor signals were converted to digital data and recorded in a PC-based portable data acquisition system. The resolution of measurement for the system can reach to 10^{-4} kine (cm/sec). In the data acquisition system, there is low-pass filter with the cut-off frequency equal to one-third of the sampling rate.

At the time of testing, only seven sensors were available and they were deployed in a 20-meter interval along the centreline of the bridge deck (see Figure 1). Owing to the limited number of sensors available, the tested bridge was divided into three segments each of 120 m long. The free vibration response in each of the three segments subjected to an impulsive force applied at the same location was measured in turn with the sensor deployments shown in Figure 1. It should be noted that the overlapped point for any two adjacent segments was used to correlate the data recorded from the three different segments.

For each sensor deployment, the impulsive force in the longitudinal (x), transverse (y) and vertical (z) directions was sequentially applied and the responses of the bridge in the same direction as that of the force were recorded. In each test, the data were recorded for a duration of

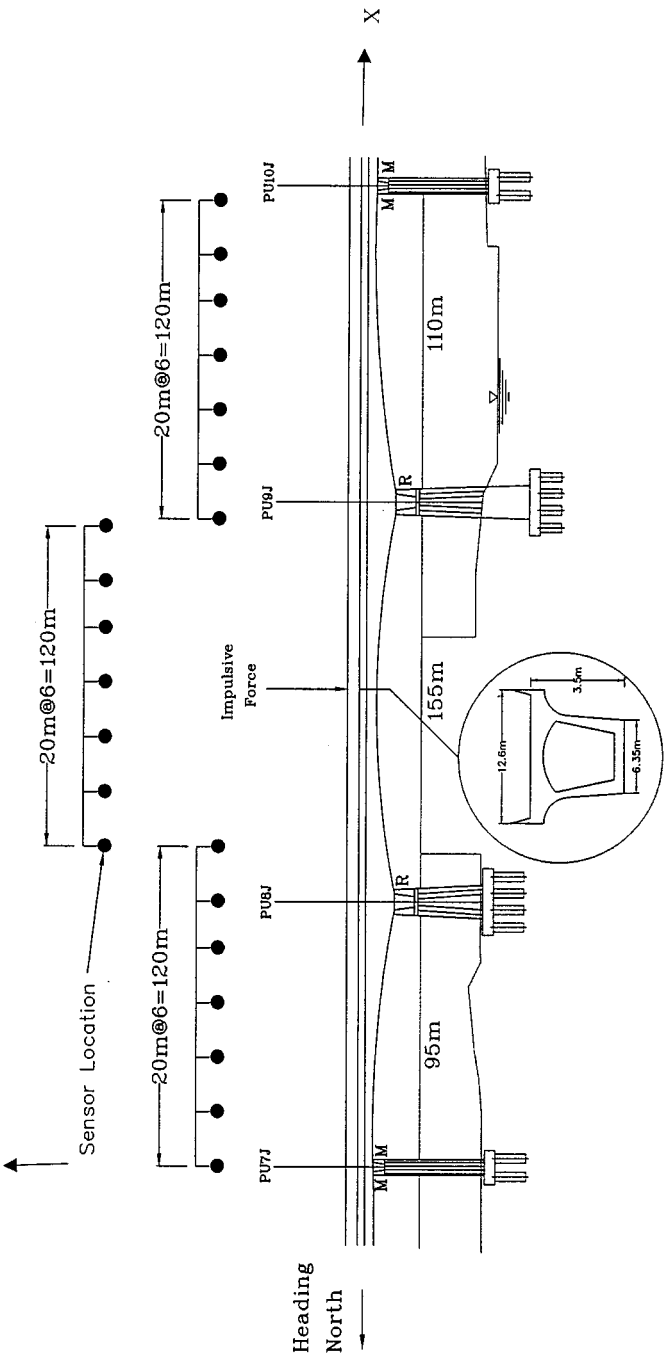

Figure 1. Northbound Yuan-Shan bridge system and sensor layout

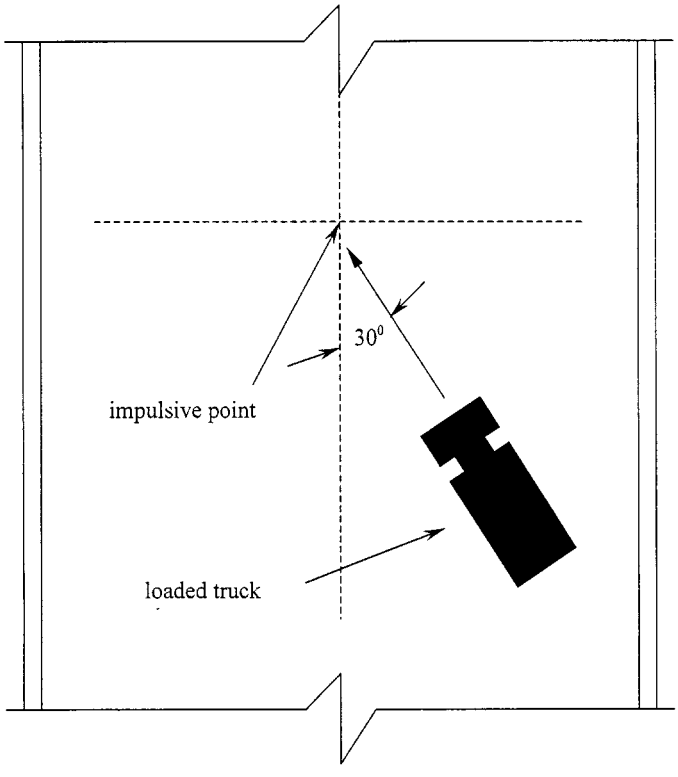

Figure 2. Impulse test in transverse direction

1 min with a sampling rate of 50 Hz. The recording time was chosen to assure that within this duration the vibration amplitude would decay to less than 2 per cent of the initial vibration amplitude. The 1-min recording time was estimated by using the bridge dynamic property provided by a finite element analysis and with the assumption that the first modal damping is 2 per cent.

3.3. Data processing

Figures 3–5 show a typical set of data recorded for the responses in three orthogonal directions at different locations subjected to the impulsive force in each direction. The responses for long elapsed time (i.e. the response in the z direction for $t > 40$ s) are mainly due to the ambient vibration. Generally speaking, the present testing procedure can produce data of better quality for the vertical and transverse directions than for the longitudinal direction in terms of free vibration to ambient vibration response ratio. Besides, the amplitude of free vibration signals decreases as the measurement location is getting farther away from the impulse point as was expected. To obtain better free vibration responses, one can move the impulse point close to the measurement stations. It is realized that the recorded data contain some contributions from the ambient vibration that cannot be separated from the free vibration responses. They were simply treated as noises in the present analysis.

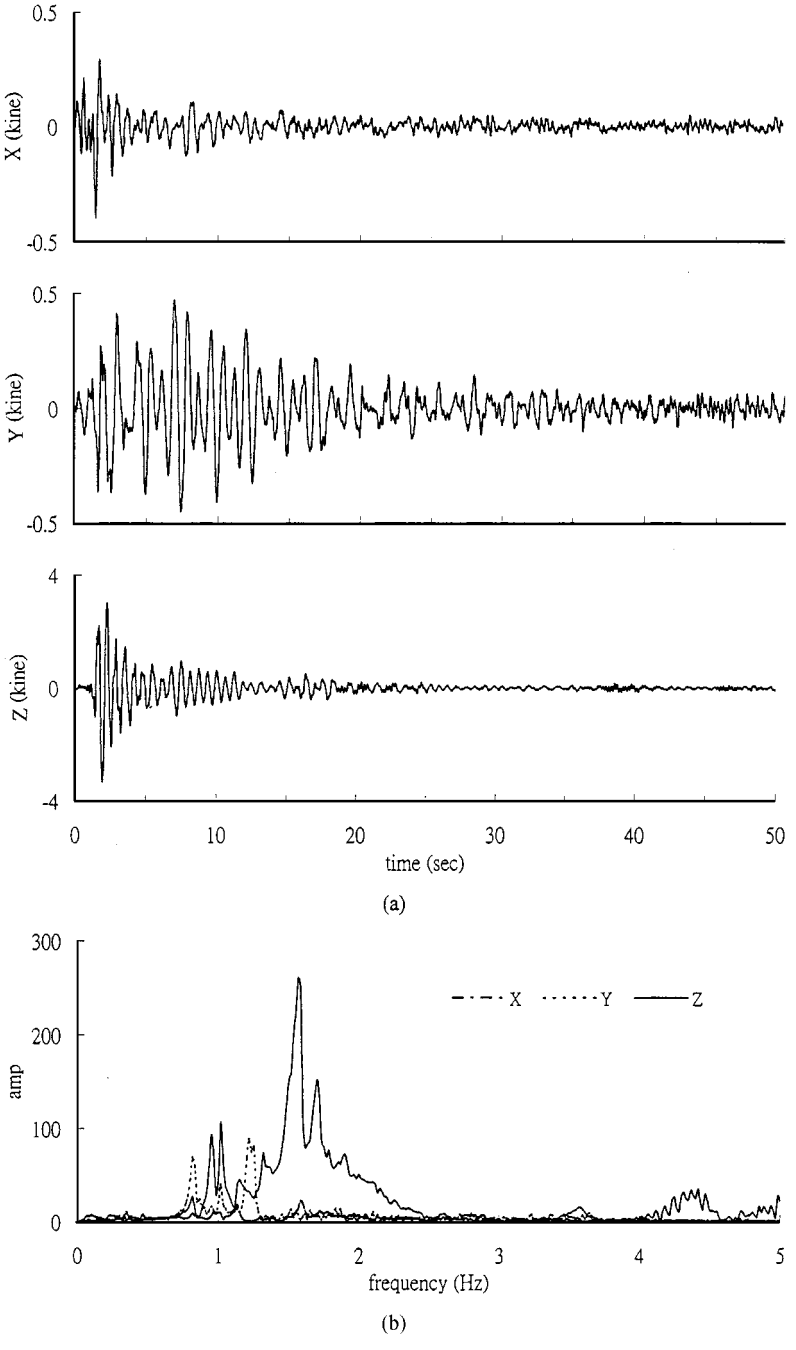

Figure 3. Impact responses at $x = 60$ m with the corresponding auto-spectra

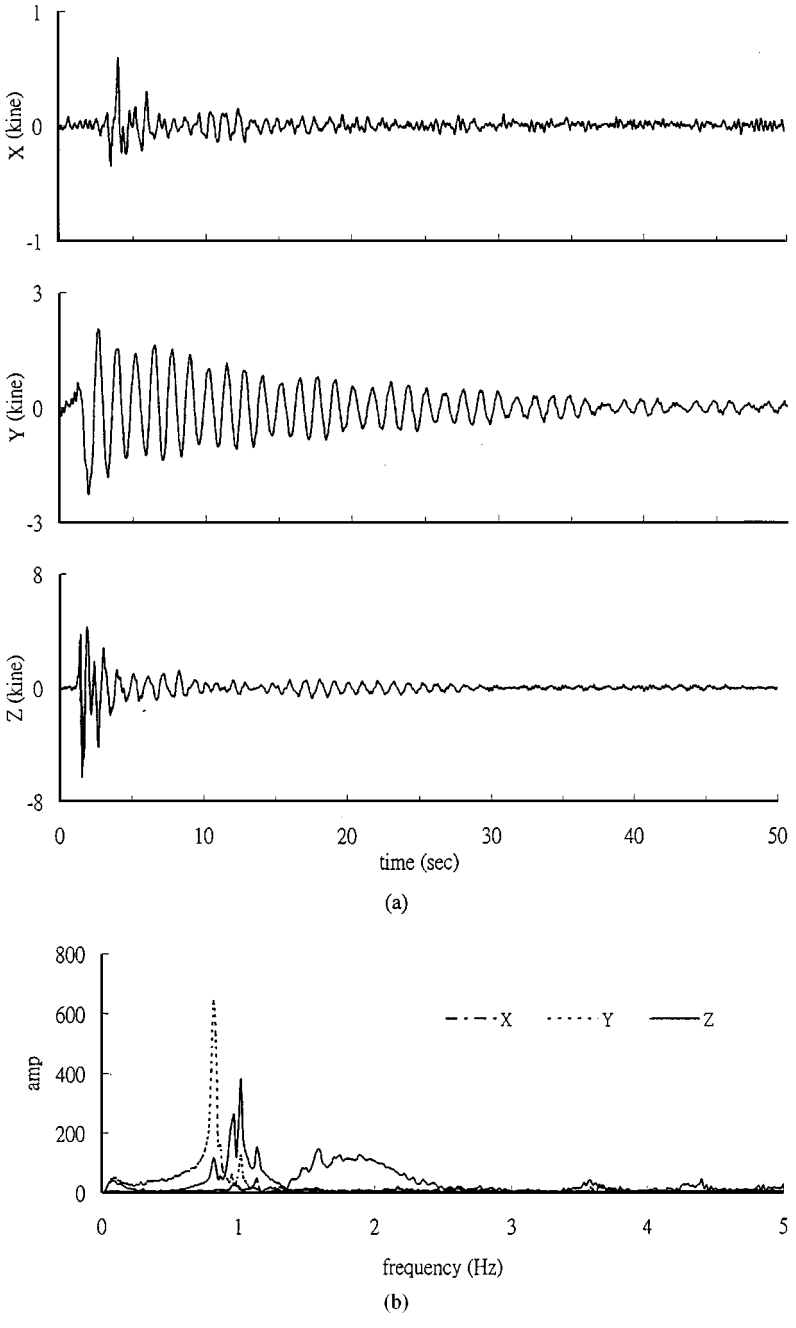

Figure 4. Impact responses at $x = 180$ m with the corresponding auto-spectra

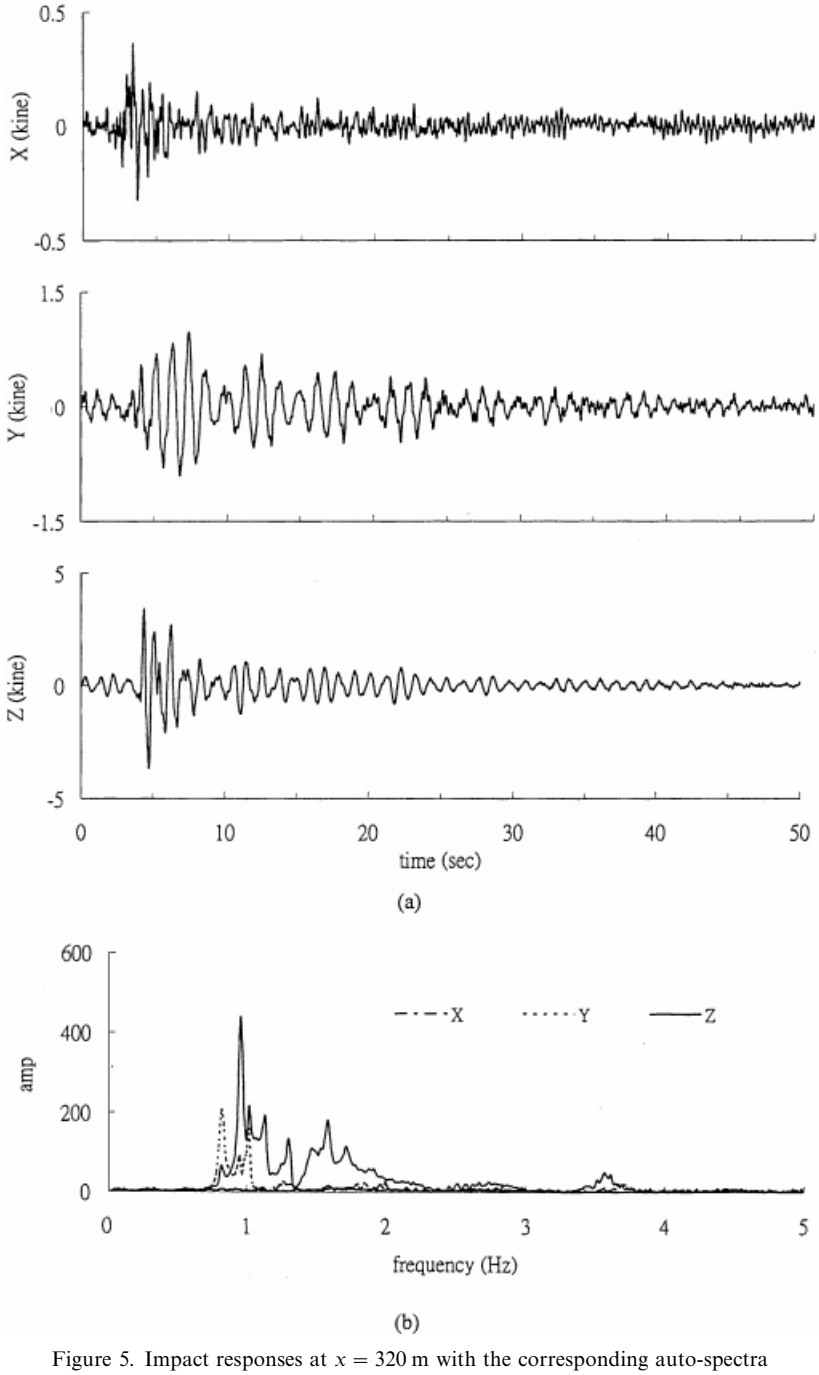

Figure 5. Impact responses at $x = 320$ m with the corresponding auto-spectra

To obtain the natural frequencies, modal damping ratios, and mode shapes from these free vibration responses, the Ibrahim Time Domain (ITD) identification technique was first applied, which was developed by Ibrahim[20] in 1973 and extensively used by Ibrahim and his co-workers[18] and others[21] to identify the dynamic characteristics of a structural system from the measured free vibration responses. This technique is suitable for treating highly coupled systems with severe modal interference, able to identify the vibration modes with rather small contribution in the response.

Based on the analytical solution of the free vibration response for a linear system, in terms of the state variables, one is able to construct a system matrix $[A]$ from the measured data in a least square sense, defined as

$$[A] = [\hat{Z}][Z]^{\mathrm{T}}([Z][Z]^{\mathrm{T}})^{-1} \tag{1}$$

where $[Z]$ and $[\hat{Z}]$ are $2m$*s matrices, with $[Z]$ representing the free vibration response of s time steps for m degrees of freedom. The dimension m is usually chosen to be larger than the total number of degrees of freedom of the system to eliminate the influence of ambient noises on the identified results. Whenever the number of stations n used to measure the free vibration responses of the system is smaller than $2m$, the data for the rows with a sequential number larger than n are filled up using a time-shift scheme described in Pappa and Ibrahim.[17] The elements in $[\hat{Z}]$differ from those in $[Z]$ by a time shift.

The eigenvectors of $[A]$ in equation (1) correspond to the mode shapes of the system under consideration in the form of state variables, while the eigenvalues of $[A]$ relate to the natural frequencies and damping ratios. The kth eigenvalue of $[A]$, which is denoted as $a_k + \mathrm{i}\, b_k$, can be related to the dynamic characteristics of the system by

$$\tilde{\beta}_k = \sqrt{\alpha_k^2 + \beta_k^2} \tag{2a}$$

$$\xi_k = -\alpha_k/\tilde{\beta}_k \tag{2b}$$

where $\tilde{\beta}_k$ is the pseudo-undamped circular natural frequency, ξ_k is the modal damping ratio,

$$\beta_k = \frac{1}{\Delta t}\tan^{-1}\left(\frac{b_k}{a_k}\right) \tag{3a}$$

$$\alpha_k = \frac{1}{2\Delta t}\ln(a_k^2 + b_k^2) \tag{3b}$$

and Δt is the time shift between $[\hat{Z}]$and $[Z]$.

The eigenvectors of $[A]$ in equation (1), which are corresponding to the mode shapes of the system, are usually complex because of the non-proportional damping nature of the system and the existence of noises in measurement. In the following application, the system is assumed to be with proportional damping and the plotted real mode shapes were deduced from the identified complex eigenvectors. The magnitude of the plotted mode shape is the magnitude of the corresponding complex eigenvector. The components of a complex eigenvector are treated as in-phase with the maximum component in the plotted mode shape if the difference of the phase angle between any component and the maximum component is between $-\pi/2$ and $\pi/2$. Otherwise, the components are treated as 180° out-of-phase from the maximum component.

Table I. Identified natural frequencies and modal damping ratios

Mode	Ambient test		Impulse test			FEM
	f (Hz)	Damping (%)	*f* (Hz)	Damping (%)	Effective mass ratio (%)	
1	0.81 (*y*)	1·3	0·80 (*y*)	1·3	67·1	0·779 (*y*)
2	0·99 (*z*)	2·9	0·96 (*x*, *z*)	3·0	0·7	0·854 (*y*)
3	1·01 (*y*)	2·0	0·99 (*y*)	2·7	13·8	0·895 (*z*)
4	1·09 (*x*)	2·1	1·10 (*x*)	3·7	87·0	0·944 (*z*)
5	1·19 (*y*)	5·3	1·23 (*y*)	5·0	17·2	1·10 (*y*)
6	1·54 (*z*)	6·9	1·52 (*x*, *z*)	5·1	29·2	1·28 (*y*)
7	1·84 (*y*)	4·6	1·84 (*y*)	4·3	0·2	1·34 (*z*)
8	2·26 (*z*)	5·5	2·15 (*z*)	6·6	8·2	1·66 (*y*)
9	2·77 (*y*)	4·7	2·51 (*x*)	4·7	0·3	1·70 (*z*)
10	3·62 (*z*)	2·0	2·73 (*y*)	4·6	0·02	2·07 (*y*)
11	3·65 (*y*)	1·6	3·56 (*z*)	1·5	0·2	2·25 (*y*)
12	4·30 (*z*)	2·2	3·66 (*y*)	1·9	1·2	2·32 (*z*)
13	—	—	4·00 (*y*)	3·2	5·5	2·50 (*x*)
14	—	—	4·36 (*z*)	1·8	15·0	3·12 (*y*)
15	—	—	—	—		3·24 (*z*)
16	—	—	—	—		3·99 (*z*)
17	—	—	—	—		4·18 (*y*)

— No identified data

The natural frequencies and modal damping ratios identified from the impulse test are listed in Table I while the modal shapes identified are shown in Figure 6. Totally, fourteen modes were identified. In Table I the alphabet parenthesized in the columns for frequencies indicates the direction(s) of the corresponding vibration mode identified from the measurement in that direction. In the legend of Figure 6, the number inside the parentheses denotes the mode number, while the alphabet represents the direction of the response that has been identified. As can be seen, the frequencies of lower modes identified in Table I correspond very well with those associated with the peaks of the auto-spectra shown in Figures 3–5. However, the frequencies for higher modes given in Table I cannot be directly identified from the auto-spectra.

It should be mentioned that, theoretically, one expects to obtain mode shapes that are coupled in the vertical (*z*), transverse (*y*), and longitudinal (*x*) directions corresponding to some natural frequencies, because the central line of the elevated bridge system is neither straight nor on the same vertical or horizontal plane. In analysis of the data from both the impulse test and ambient test, we did find that some natural frequencies were repeatedly identified from some sets of measurement in different directions. Note that only those mode shapes that can be completely identified have been shown in Figure 6. Although no modes completely coupled in *x*, *y* and *z* directions were identified, it is believed that most of the mode shapes in the dominant direction for each mode were identified.

The effective mass ratio[22] for each identified mode is also given in Table I. In computing the effective mass ratios, the lumped mass matrix corresponding to the observation stations was established based on the design data. Since no complete coupling modes in the three directions were identified, the identified mode shapes in each direction are assumed to be uncoupled in computing the effective mass ratios. Although the mode shapes were identified to be related to both the *x* and *z* directions for the second and sixth modes, only the effective mass in the

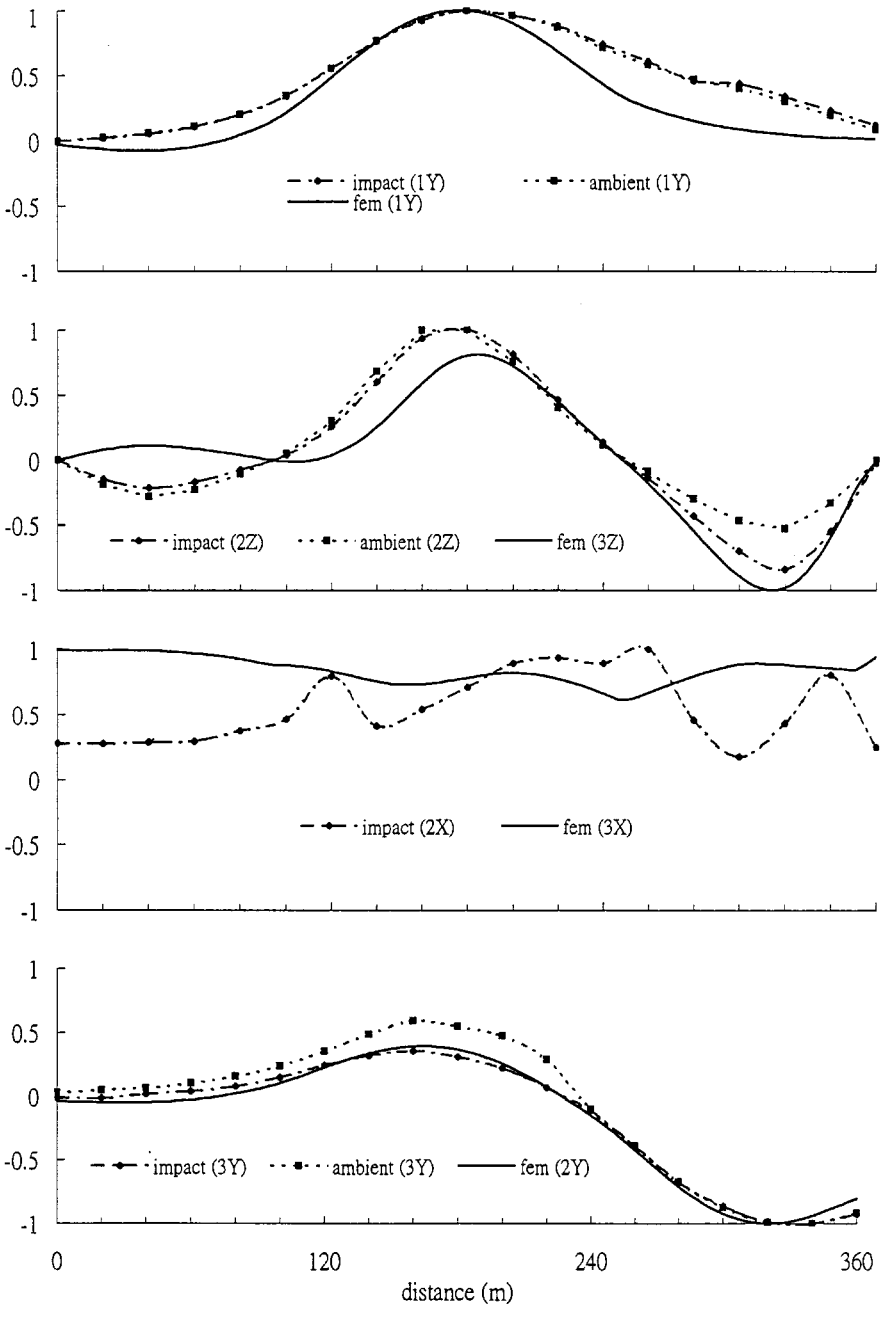

Figure 6. Comparison of identified mode shapes with finite-element results

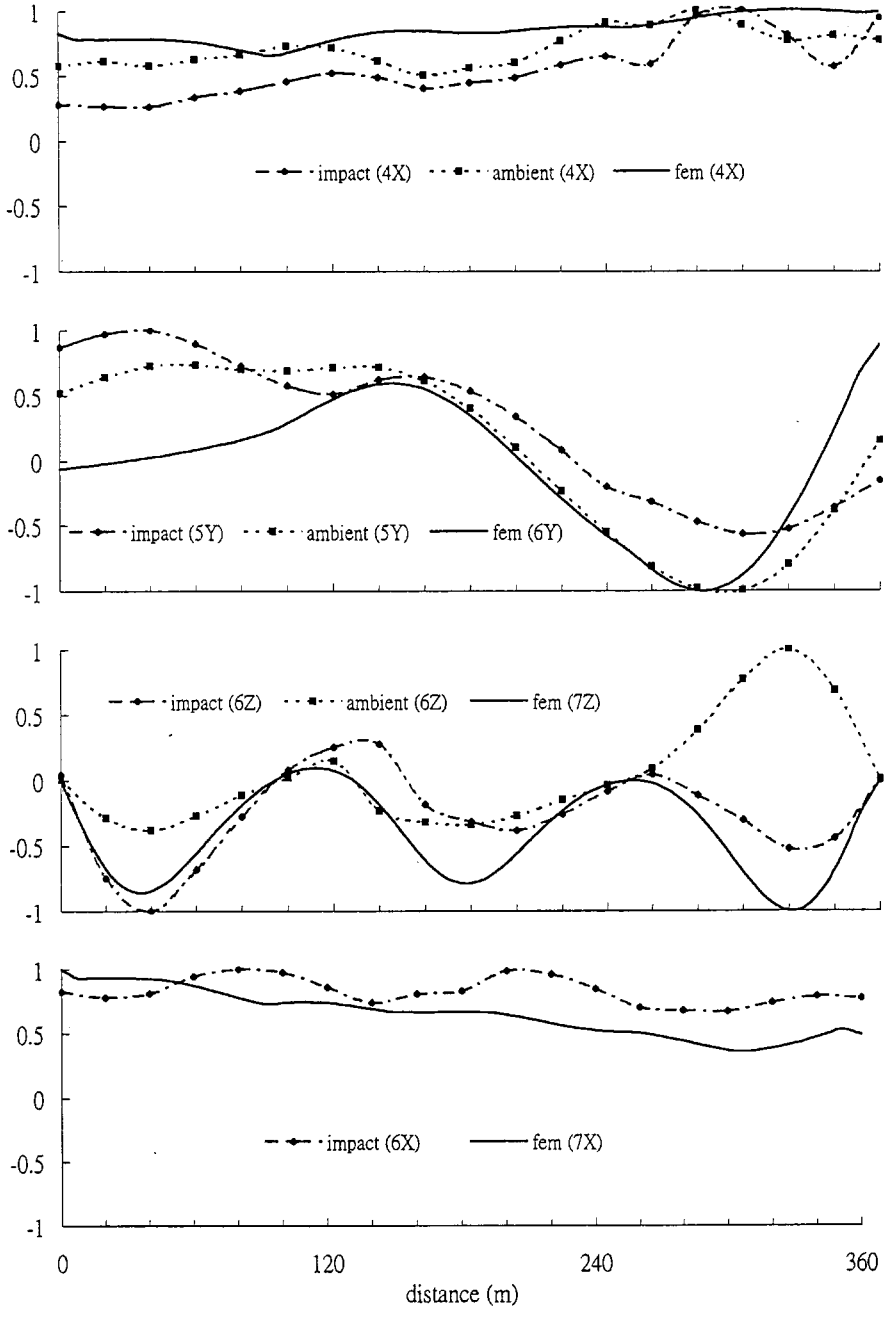

Figure 6. Continued

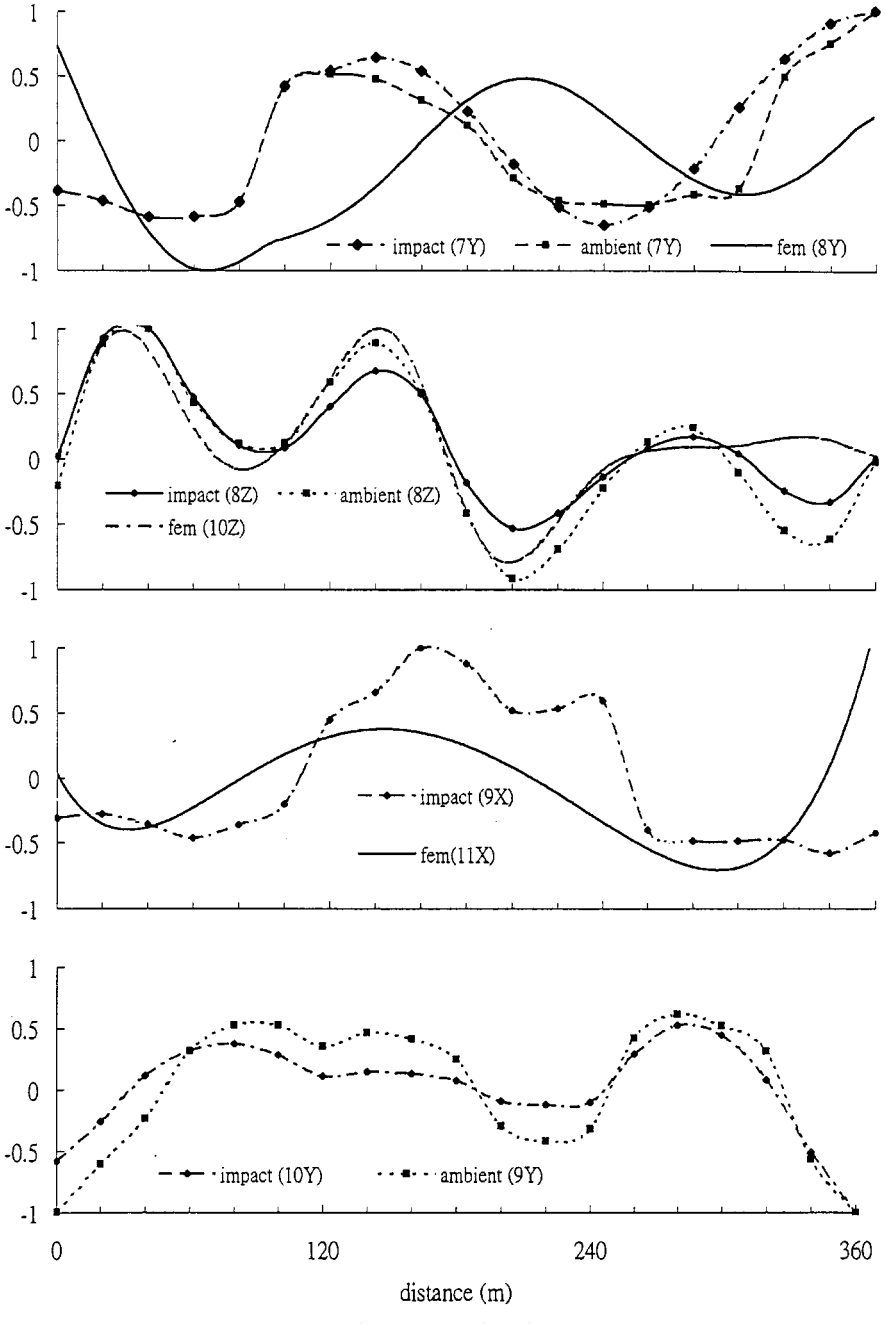

Figure 6. Continued

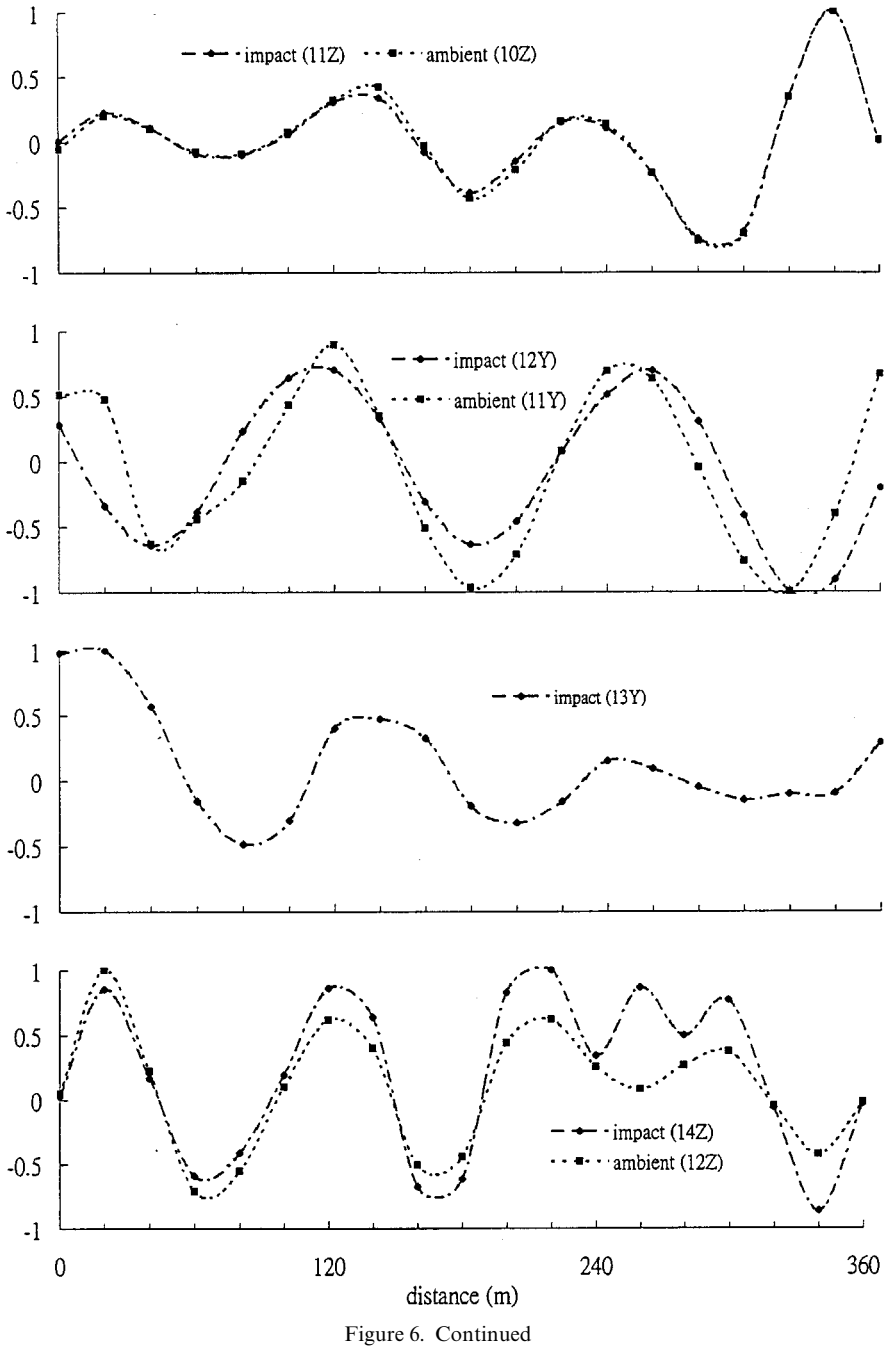

Figure 6. Continued

dominant direction for each of the two modes, which was judged based on the finite element results, was computed. The accumulated effective mass ratio for the first three modes in the y-direction is close to 100%, and the effective mass ratio for the first mode in the x-direction is considered predominant (as large as 87 per cent). In comparison, the effective mass for the mode in z-direction is not concentrated in one or few modes only. The sum of the effective mass ratios for all the identified modes in the z-direction (five modes) accounts for only 53·3 per cent. It should be noted that the sum of the effective mass ratios for the modes in the y-direction is slightly over 100 per cent, which may be attributed to the inconsistency between the estimated lumped mass matrix and that implied by the identified mode shapes and due to the assumption of completeness in the identified mode shapes.

4. AMBIENT VIBRATION TEST

4.1. Instrumentation for measurement

The measurement set-up for ambient vibration tests is the same as that for free vibration tests. Using the same sensor layout, each ambient vibration measurement was taken immediately after one impulse test was completed for one direction. However, in order to obtain better identified results, the number of recorded data from each sensor has been significantly increased, compared with that for free vibration tests. For each measurement, the responses of the bridge were recorded for a duration of 7 min with 50 Hz sampling rate.

4.2. Analysis of data

The recorded velocity data of seven channels from each set of measurement in the ambient test were processed through the random decrement (Randomdec) technique[19]. Then, the ITD identification technique was applied to these Randomdec signatures to extract the natural frequencies, modal damping ratios, and mode shapes for the system.

Without any meticulous mathematical proof but with physical intuition, Cole[16] originally introduced the Randomdec technique in 1971 to study the application of correlation functions to measurement of damping and damage assessment in aircraft structures. Yang and his colleagues[23,24] further developed this technique to enhance identification of modal parameters. Nevertheless, a rigorous mathematical proof on the equivalence between the random signals of a system through the Randomdec technique and the free decayed responses of the system was not proposed until 1982 by Vandiver *et al.*[25]

Basically, the Randomdec technique is a signal processing technique for obtaining ensemble averages of pre-selected segments of random response signals. Assume that $\{X(t)\}$ and $\{Y(t)\}$ are two stationary random processes, and that $x(t)$ and $y(t)$ shown in Figure 7 are two samples of $\{X(t)\}$ and $\{Y(t)\}$, respectively. If a threshold level, x_s, is chosen, and $x(t_i) = x_s$ for $i = 1, 2, \ldots, N$ are found from the measured data, then the Randomdec technique gives the signals defined as (see Figure 7)

$$\delta_{xx}(\tau) = \frac{1}{N} \sum_{i=1}^{N} x(t_i + \tau) \tag{4a}$$

$$\delta_{xy}(\tau) = \frac{1}{N} \sum_{i=1}^{N} y(t_i + \tau) \tag{4b}$$

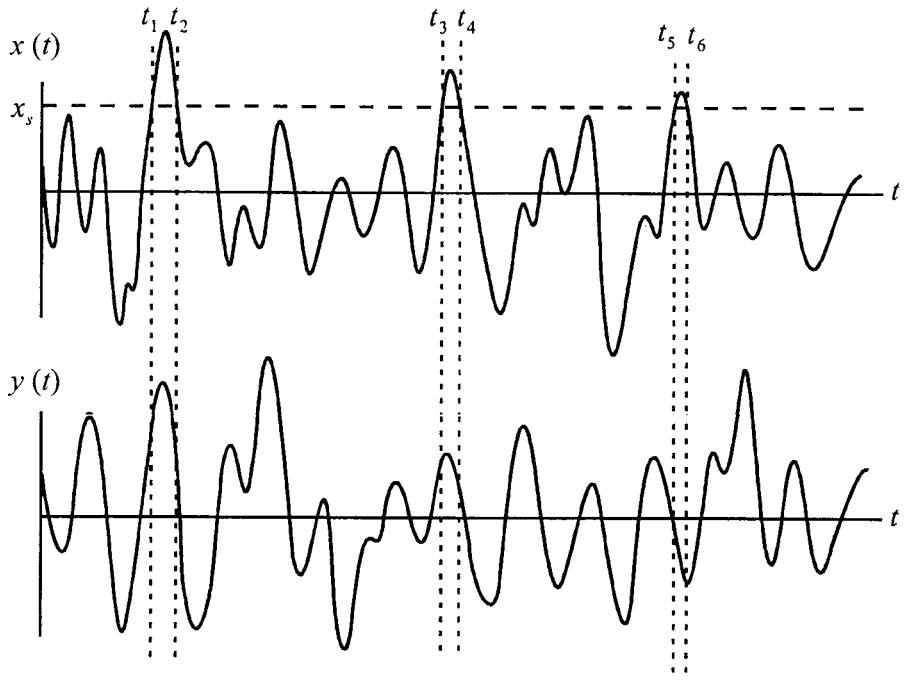

Figure 7. Construction of Randomdec signatures

where, $\delta_{xx}(\tau)$ is the unbiased estimation of auto-Randomdec signature of $x(t)$, and $\delta_{xy}(\tau)$ is the unbiased estimation of the cross-Randomdec signature of $y(t)$ with respect to $x(t)$.

Vandiver *et al.*[25] and Huang and Yeh[26] proved that the estimation given by equation (4) is unbiased, and the variances of the estimation are proportional to the variances of the raw data but inversely proportional to N in equation (4). That is why we need a longer record for the ambient vibration test. Furthermore, Huang and Yeh[26] proved that if the input forces for a time-invariant linear system with non-proportional damping are a Gaussian white noise vector process without a phase-shift relationship among the components, then the Randomdec displacement or velocity signatures are equivalent to the free decayed responses of the system. However, the equivalent relationship does not remain valid for the Randomdec acceleration signature.

A set of typical measured velocity data with the corresponding auto-spectra from the ambient test and the resultant Randomdec velocity signatures are shown in Figure 8. As can be seen, the Randomdec signatures resemble free decayed signals. The ITD technique was then applied to the Randomdec signatures to determine the dynamic characteristics of the bridge. Totally, twelve modes were identified from the ambient vibration test. For comparison, the natural frequencies and modal damping ratios identified are also listed in Table I. Besides, the modal shapes identified that appear to be similar to those of the free vibration tests are also plotted in Figure 6. Although the seventh mode shape in y-direction was not completely identified, it is still given in Figure 6 simply to show its existence. By comparing the frequencies identified with those corresponding to peaks of the auto-spectra shown in Figure 8, one can observe that they are consistent. However, identifying the natural frequencies for higher modes, mode shapes, and damping ratios from the auto-spectra alone is not an easy task.

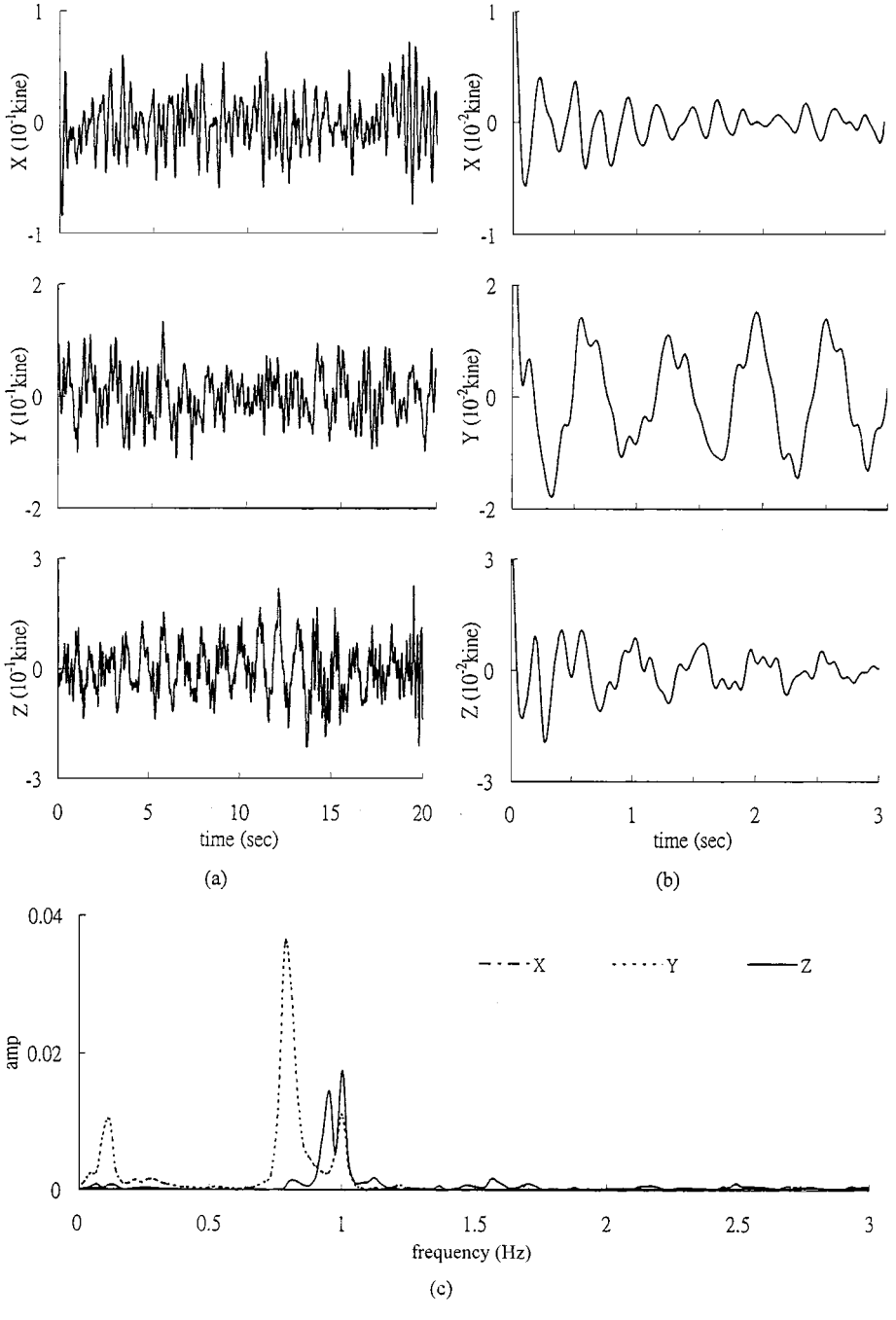

Figure 8. (a) A typical ambient vibration responses at $x = 180$ m; (b) corresponding Randomdec signature; and (c) auto-spectra

5. COMPARISON OF THE IDENTIFIED RESULTS WITH FINITE ELEMENT RESULTS

5.1. Finite element results

The finite element results shown in Table I and Figure 6 were obtained by the commercial finite element package SAP90, using in particular the beam element that has six degrees of freedom at each node. In the finite element modelling, 89 beam elements were used for modelling the superstructure and 20 beam elements were used for the piers. These beam elements are assumed to be uniform cross-section. Designed material properties, E (Young's modulus) $= 2{\cdot}806 \times 10^6$ kN/m^2 and G (shear modulus) $= 1{\cdot}167 \times 10^6$ kN/m^2, were used in this analysis. The soil–structure interaction was considered by using equivalent soil springs connected to the pile cap for each pier of the bridge.[27] Each of equivalent soil springs represents the stiffness of the rigid pile cap, assumed to be massless, associated with the movement in each of the three orthogonal directions or the rotation about each of the three orthogonal axes. Consequently, six frequency independent soil springs were established following the FHWA report by Lame and Martin.[28]

For comparison with measured results, the first seventeen natural frequencies computed from the finite element analysis are listed in Table I as well, in which the dominant direction of vibration is determined from the maximum component of each eigenvector (see Table II). In contrast, only the modal shapes that are judged to be similar to the measured ones have been plotted in Figure 6.

Since the central line of the elevated bridge system is neither straight nor on the same vertical or horizontal plane, the mode shapes computed appear to be coupled in the vertical, transverse, and longitudinal directions. To show the coupling strength in each mode, Table II lists the ratios of the maximum component in each direction to the maximum component of the corresponding

Table II. Ratios of maximum component in each direction to maximum modal component

Mode	X_{max}/D_{max}	Y_{max}/D_{max}	Z_{max}/D_{max}
1	0·055	1·000	0·312
2	−0·068	1·000	−0·390
3	−0·152	0·439	1·000
4	−0·288	0·208	1·000
5	0·075	1·000	−0·045
6	0·217	1·000	−0·390
7	0·249	0·204	1·000
8	−0·082	1·000	−0·077
9	−0·303	0·060	1·000
10	0·105	1·000	0·058
11	0·511	1·000	0·007
12	0·218	−0·035	1·000
13	1·000	−0·052	−0·001
14	−0·125	1·000	−0·046
15	−0·113	−0·022	1·000
16	0·174	−0·026	1·000
17	0·115	1·000	−0·008

eigenvector. Indeed, most of the vibration modes show a strong coupling between the responses in different directions.

5.2. *Comparison of results*

The first observation from Table I is that most of the frequencies identified from the ambient vibration test show an excellent agreement with those from the impulse test. The frequencies of the first seven modes are less than 2 Hz, implying that no severe interaction can occur between the bridge and the running vehicles, whose resonant frequencies lie generally in the 2–5 Hz range. From this point, the bridge is considered well designed. For the first three modes, the natural frequencies identified from the impulse tests appear to be only slightly smaller than those from the ambient vibration tests, even though the magnitude of response for the former is much larger than that for the latter. It should be noted that the ninth and thirteen modes from the impulse test do not have their correspondence from the ambient test.

The other observation from Table I is that the natural frequencies computed from the finite element program generally do not match well with the ones identified from the tests. In particular, the analytical frequencies of the first modes in different main directions are somewhat smaller than the identified ones. It is possible that the indicated direction of the identified mode shape may not be the real dominant direction of the mode. For example, the identified fourth mode was obtained from the measurement for the x-direction, while the dominant direction of the fourth mode has been analytically shown to be the z-direction. They seem inconsistent. However, in the identification process, we did find the same frequency from two of the three sets of measurement in the z-direction. From the auto-spectrum of the z-direction responses shown in Figures 3–5, one can also observe that there is a peak corresponding to the frequency around 1·1 Hz.

For comparison, the vibration modes solved by the finite element method that appear to have their correspondence with the measured ones are also plotted in Figure 6. The fifth analytical mode was excluded from Figure 6, since its vibration shapes does not match any of the modes identified experimentally. The lack of consistency between the analytical and experimental results can be attributed mainly to the difference between the real structure and the finite element model, concerning the geometric and material properties, and boundary conditions. As a matter of fact, the results from the field tests serve as a useful basis for calibrating the finite element model.

The level of consistency for the modal damping ratios identified from the two types of tests is not so good as that for the natural frequencies, but appear to be reasonably acceptable (see Table I). Most of the damping ratios identified from the tests are smaller than the design value of 5 per cent. They do not show the trend of increasing with the increase of natural frequency. Furthermore, the damping ratio for the first horizontal mode does not exceed that for the first vertical mode, which is not consistent with what Shepherd and Sidwell[29] observed from their measurement for bridges of the straight beam type. The reason is likely due to that the vibration modes are basically coupled in three orthogonal directions so that even for the modes dominated by the vertical vibration, significant damping will be contributed by the piers through the soil–structure interaction.

To evaluate the correlation of the mode shapes obtained by different methods, the index MAC (modal assurance criterion)[30] is computed to show the correlation between any two mode shapes

Table III. MAC values for the modal shapes obtained from different methods

Free vibration test vs. ambient vibration test			Free vibration test vs. finite element analysis		
Direction	Mode No. free/ambient	MAC	Direction	Mode No. free/FEM	MAC
Y	1/1	0·999	*Y*	1/1	0·805
Z	2/2	0·955	*Z*	2/3	0·766
Y	3/3	0·953	*X*	2/3	0·526
X	4/4	0·930	*Y*	3/2	0·980
Y	5/5	0·807	*X*	4/4	0·820
Z	6/6	0·000	*Y*	5/6	0·048
Y	7/7	0·646	*Z*	6/7	0·586
Z	8/8	0·914	*X*	6/7	0·883
Y	10/9	0·847	*Y*	7/8	0·010
Z	11/10	0·993	*Z*	8/10	0·675
Y	12/11	0·655	*X*	9/11	0·018
Z	14/12	0·821	—	—	—

— means that no suitable modal shape is found from finite element analysis, which is similar to that from free vibration test

of interest, which is defined as

$$\mathrm{MAC}(\phi_{i\mathrm{I}}, \phi_{i\mathrm{A}}) = \frac{|\{\phi_{i\mathrm{I}}\}^{\mathrm{T}}\{\phi_{i\mathrm{A}}\}^{*}|^2}{\{\phi_{i\mathrm{I}}\}^{\mathrm{T}}\{\phi_{i\mathrm{I}}\}^{*}\{\phi_{i\mathrm{A}}\}^{\mathrm{T}}\{\phi_{i\mathrm{A}}\}^{*}} \tag{5}$$

where $\{\phi_{i\mathrm{I}}\}$ is the ith mode shape identified from the impulse test, and $\{\phi_{i\mathrm{A}}\}$ is the corresponding mode shape obtained from the ambient vibration test or finite element analysis. The superscript $*$ in equation (5) denotes the conjugate. Apparently, two corresponding modes are considered well correlated if the MAC value is close to one, and uncorrelated if close to zero.

The values of MAC for the modal shapes identified from the free vibration and ambient vibration tests are given in Table III. In general, the mode shapes identified from both types of tests appear to match each other very well (see Figure 6), as indicated by the high values of MAC. One exception is the sixth mode, for which the MAC value is equal to zero. For this mode, the vibrational shapes of the first two spans are consistent with each other, but those of the third span are just out-of-phase. Such a discrepancy can be attributed to the fact that the measurement reference point for the third span was set right on the pier. Because the vertical response of this reference point is so small, compared with those at the other locations, the phase angle of the mode shape identified at this point may not be reliable for some cases. To resolve this difficulty, one had better use two reference points for each set of tests.

Table III also lists the MAC values for the modal shapes obtained from the free vibration test and finite element analysis. As can be seen, generally good correlation exists between the two sets of modal shapes, especially for the first four modes.

6. CONCLUDING REMARKS

This paper has presented a free vibration testing procedure for a multi-span freeway bridge by using a loaded truck to generate impulsive forces, which can be easily set up and carried out. The

measurement indicates that the proposed testing procedure provides good quality of free vibration responses. By applying the Ibrahim time-domain identification technique to the recorded free vibration responses, one can easily and accurately identify the frequencies, damping ratios, and modal shapes of the bridge up to the first fourteen modes.

For the purpose of verification, ambient vibration tests were also conducted, from which the data were processed through the random decrement technique combined with the Ibrahim time-domain identification technique. The dynamic characteristics of the bridge for the first twelve modes identified from the ambient vibration test correlated excellently with those from the free vibration test. Although much more modes can be identified from the free vibration test than from the ambient test, because of the higher quality of data generated by the former, the easiness and great applicability of the ambient vibration test can still be appreciated.

Comparison of the measured results with the finite element solution shows a reasonable match for the first four modes, especially for the vibration shapes. Some of the first seventeen modes obtained from finite element analysis do not have their matching modes from the test results. This is an indication that the finite element model used in the structure design needs further refinement, through a more realistic evaluation of the boundary conditions, geometric and material properties of the bridge (i.e. the constants for soil springs, the non-uniform cross-section of box girder, and the real Young's modulus) by experiments or by model updating techniques.[31]

ACKNOWLEDGEMENTS

The research reported herein was sponsored by the Taiwan-Area National Freeway Bureau, Ministry of Transportation and Communications, through a five-year research project for monitoring the Yuan-Shan Bridge.

REFERENCES

1. J. H. Rainer and A. VanSelst, 'Dynamic properties of Lions Gate Bridge', *Proc. Conf. on Dynamic Response of Structures: Instrumentation, Testing Methods and System Identification*, ASCE Specialty Conf., University of California, 1976, pp. 243–252.
2. J. H. Rainer and G. Pernica, *Dynamic Testing of a Modern Concrete Bridge*, National Research Council of Canada, 1979, pp. 447–455.
3. A. Nishimura and H. Haya, 'Assessment of the structural integrity of bridge foundation by the impact vibration test', GEO-COAST, Yokohama, 1991, pp. 719–724.
4. R. Shepherd and G. K. Sidewell, 'Investigations of the dynamic properties of five concrete bridges', *4th Australian Conf. on the Mechanics of Structures and Materials*, University of Queensland, Brisbane, Australia, 1977, pp. 261–268.
5. R. Eyre, 'Dynamic tests on the Cleddau Bridge at Milford Haven', *Supplementary Report 200UC*, Transport and Road Research Laboratory, Department of Environment, Crowthorne, United Kingdom, 1976.
6. B. M. Dougla, C. D. Drown and M. L. Gordon, 'Experimental dynamics of highway bridges', in G. Hart (ed.) *Proc. Specialty Conf. on Dynamic Response of Structures, Experimentation, Observation, Prediction and Control*, ASCE, New York, 1981, pp. 698–712.
7. V. R. Mclamore, G. C. Hart and I. R. Stubbs, 'Ambient vibration of two suspension bridge', *J. Struct. Div. ASCE* **97** (ST10), 2567–2583 (1971).
8. P. T. Y. Chang, C. C. Chang and L. D. Zhu, 'A streamlined ambient vibration analysis program for long-span bridges', *Proc. 6th East Asia-Pacific Conf. on Structural Engineering and Construction*, Taipei, Taiwan, 1998, pp. 375–380.
9. S. M. LaShomb, 'Bridge vibration', *M.S. Thesis*, University of Connecticut, Storrs Connecticut, 1985.
10. D. F. Mazurek, 'Monitoring structural integrity of girder bridges through vibration measurement', *Ph.D. Dissertation*, University of Connecticut, Storrs Connecticut, 1989.
11. Y. B. Yang, I. C. Tsai, C. C. Kao, C. S. Huang and L. Y. Lu, 'Dynamic and static minitoring and aalysis of Si-Tsang bridge', *First Mid-term Report to Bureau of Civilian Housing and City Planning*, Taipei, Taiwan, R.O.C., 1994 (in Chinese).
12. P. Paultre, O. Chaallal and J. Proulx, 'Bridge dynamic and dynamic amplification factors—a review of analytical and experimental findings', *Can. J. Civil Engng.* **19**(2), 260–278 (1992).

13. D. A. Schoenwald, 'System identification using a wavelet-based approach', *Proc. 32nd IEEE Conf. on Decision and Control*, San Antionio, TX, USA, 1993, pp. 3064–3065.
14. A. N. Robertson, K. C. Park and K. F. Alvin, 'Identification of structural dynamic models using wavelet-generated impulse response data', *Proc. 1995 ASME Design Engineering Technical Conf.*, Boston, MA, USA, 1995, pp. 1335–1344.
15. M. Ruzzene, A. Fasana, L. Garibaldi and B. Piombo, 'Natural frequencies and damping identification using wavelet transform: application to real data', *Mech. Systems Signal Process.* **11**(2), 207–218 (1997).
16. H. A. Jr. Cole, 'Method and apparatus for measuring the damping characteristics of a structure', *United State Patent No. 3,620,069,* 1971.
17. R. S. Pappa and S. R. Ibrahim, 'A parametric study of the Ibrahim time domain modal identification algorithm', *Shock Vib. Bull.* **51**(3), 43–72 (1981).
18. S. R. Ibrahim and R. S. Pappa, 'Large modal survey testing using the ibrahim time domain identify technique', *AIAA J. Spacecraft Rockets* **19**(5), 459–465 (1982).
19. C. S. Huang, I. C. Tsai and C. H. Yeh, 'Application of random decrement technique to identify the characteristics of a building in time domain from ambient vibration measurement', *J. Chinese Inst. Civil Hydraulic Engng.* **10**(3), 537–547 (1998).
20. S. R. Ibrahim and E. C. Mikulcik, 'A time domain modal vibration test technique', *Shock Vib. Bull.* **43**(4), 21–37 (1973).
21. P. C. Lin and C. P. Tang, 'The vibration measurement and the system identification of the teaching building of I-Lan Institute of Agriculture and Technology: Part II', *NSC Report No. 82-0414-p033*-001-*B*, *National Science Council, R.O.C.*, 1993.
22. A. K. Chopra, *Dynamics of Structures*, Prentice-Hall, Englewood Cliffs, NJ, 1995.
23. J. C. S. Yang and D. Caldwell, 'Measurement of damping and the detection of damages in structures by the random decrement technique', *Shock Vib. Bull.* **46**, 129–136 (1976).
24. J. C. S. Yang, G. Z. Qi, A. J. Durelli, L. Esteva and V. Pavlin, 'In-situ determination of soil damping in the lake deposit area of Mexico City', *Soil Dyn. Earthquake Engng.* **8**(1), 43–52 (1989).
25. J. K. Vandiver, A. B. Dunwoody, R. B. Campbell and M. F. Cook, 'A mathematical basis for the random decrement vibration signature analysis technique', *J. Mech. Des.* **104**, 307–313 (1982).
26. C. S. Huang and C. H. Yeh, 'Some properties of randomdec signatures', *Mech. System Signal Process.* (1999) accepted.
27. I. C. Tsai and J. C. Yang, 'Dynamic analysis of a freeway bridge subjected to earthquake', in 'Dynamic and Static Monitoring and Analysis of Yuan-Shan Bridge', *2nd Report to National Freeway Bureau*, Ministry of Transportation and Communication, Taiwan, 1996 (in Chinese).
28. I. Lame and G. R. Martin, 'Seismic design of highway bridge foundation', *FHWA Report No. FHWARD-86/101,* Virginia, U.S.A., 1986.
29. R. Shepherd and G. K. Sidwell, 'Investigations of the dynamic properties of five concrete bridges', *4th Australian Conf. on the Mechanics of Structures and Materials*, Brisbane, Australia, 1977, pp. 261–268.
30. D. J. Ewins, *Modal Testing: Theory and Practice*, Wiley, New York, 1985.
31. J. E. Mottershead and M. I. Friswell, 'Model updating in structural dynamics: a survey', *J. Sound Vib.* **167**(2), 347–375 (1993).

